ACS OMEGA

Article

Cite This: ACS Omega XXXX, XXX, XXX−XXX

http://pubs.acs.org/journal/acsodf

Residue Network Involved in the Allosteric Regulation of Cystathionine β-Synthase Domain-Containing Pyrophosphatase by Adenine Nucleotides

Viktor A. Anashkin,[†] Anu Salminen,[‡] Ekaterina Osipova,[†] Svetlana A. Kurilova,[†] Ilia D. Deltsov,[†] Reijo Lahti,[‡] and Alexander A. Baykov*[,†]

[†]Belozersky Institute of Physico-Chemical Biology and Department of Chemistry, Lomonosov Moscow State University, Moscow 119899, Russia

[‡]Department of Biochemistry, University of Turku, FIN-20014 Turku, Finland

Supporting Information

ABSTRACT: Inorganic pyrophosphatase containing regulatory cystathionine β-synthase (CBS) domains (CBS-PPase) is inhibited by adenosine monophosphate (AMP) and adenosine diphosphate and activated by adenosine triphosphate (ATP) and diadenosine polyphosphates; mononucleotide binding to CBS domains and substrate binding to catalytic domains are characterized by positive cooperativity. This behavior implies three pathways for regulatory signal transduction — between regulatory and active sites, between two active sites, and between two regulatory sites. Bioinformatics analysis pinpointed six charged or polar amino acid residues of *Desulfitobacterium hafniense* CBS-PPase as potentially important for enzyme regulation. Twelve mutant enzyme forms were produced, and their kinetics of pyrophosphate hydrolysis was measured in wide concentration ranges of the substrate and various adenine nucleotides. The parameters derived from this analysis included catalytic activity, Michaelis constants for two active sites, AMP-, ATP-, and diadenosine tetraphosphate-binding constants for two regulatory sites, and the degree of activation/inhibition for each nucleotide. Replacements of arginine 295 and asparagine 312 by alanine converted ATP from an activator to an inhibitor and markedly affected practically all the above parameters, indicating involvement of these residues in all the three regulatory signaling pathways. Replacements of asparagine 312 and arginine 334 abolished or reversed kinetic cooperativity in the absence of nucleotides but conferred it in the presence of diadenosine tetraphosphate, without effects on nucleotide-binding parameters. Modeling and molecular dynamics simulations revealed destabilization of the subunit interface as a result of asparagine 312 and arginine 334 replacements by alanine, explaining abolishment of kinetic cooperativity. These findings identify residues 295, 312, and 334 as crucial for CBS-PPase regulation via CBS domains.

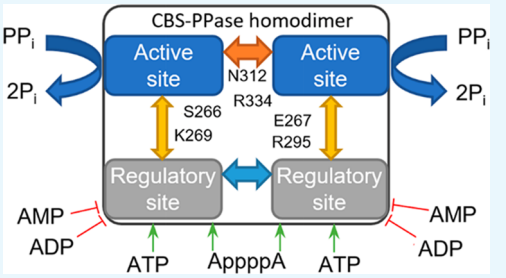

INTRODUCTION

Regulatory CBS domains are found in many important enzymes, membrane transporters, and other proteins in all kingdoms of life and in most cases bind adenine nucleotides as regulatory ligands.[1,2] The human genome encodes 75 CBS domain-containing proteins, and mutations in some of them are associated with hereditary diseases.[3,4] However, surprisingly little is known about the mechanism of CBS domain-mediated regulation, mainly because of difficulty in obtaining structural data for full-size proteins. In this regard, prokaryotic CBS domain-containing pyrophosphatase (CBS-PPase) may be a good model to study this phenomenon because it is easily accessible and stable, binds an array of adenine nucleotides, including diadenosine polyphosphates, and has a relatively simple structure; its activity can be conveniently and precisely measured. An additional merit of CBS-PPase is that its regulation through CBS domains is not complicated by other regulatory mechanisms, such as autophosphorylation in AMP-activated protein kinase[5] and dithiol reduction/oxidation in cystathionine β-synthase.[6]

CBS-PPases belong to family II PPases—homodimeric Co or Mn metalloenzymes[7,8] with the most complex domain organization among different PPases. Each subunit of canonical family II PPase is formed by two catalytic domains, DHH and DHHA2,[9,10] which are supplemented by regulatory domains in CBS-PPases.[8] An ∼250-residue regulatory insert, found within the DHH domain, generally consists of a pair of cystathionine β-synthase (CBS) domains (a Bateman module[11]) intercalated by a DRTGG domain. The crystal structure of the isolated regulatory insert indicates that four CBS domains belonging to two Bateman modules form a disk-like structure at the subunit interface.[12] By binding to the Bateman module, AMP and ADP inhibit CBS-PPase, whereas ATP and linear diadenosine

Received: June 24, 2019
Accepted: August 28, 2019

DOI: 10.1021/acsomega.9b01879
ACS Omega XXXX, XXX, XXX−XXX

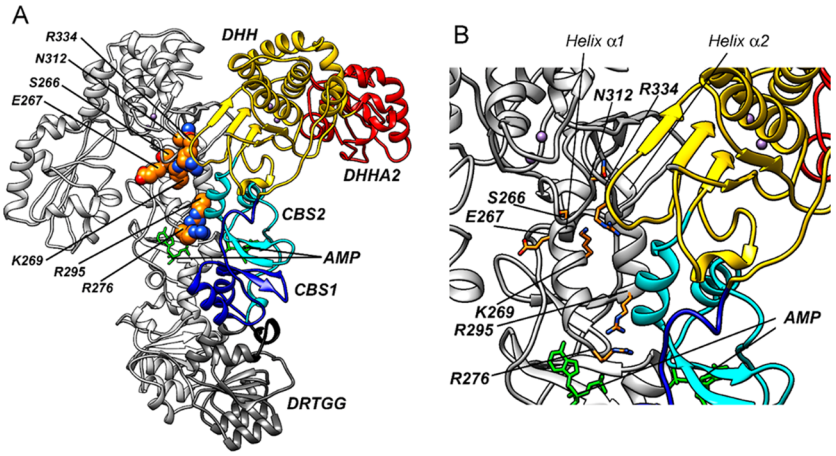

Figure 1. Predicted three-dimensional structure of *dh*PPase dimer. The structure was obtained by homology modeling using the structures of canonical *B. subtilis* PPase (DHH and DHHA2 domains, PDB ID: 1 K23) and the regulatory part of *cp*PPase (CBS1, CBS2, and DRTGG domains, PDB ID: 3 L31) as the templates. The domains are shown in different colors in one subunit; the other subunit is gray. AMP molecules bound in the regulatory parts are depicted in green, and two Mn^{2+} ions bound in both active sites are shown as violet spheres. (A) The model of the whole enzyme dimer. The residues selected for replacements or replaced previously (R276) are shown in a spherical representation in the subunit colored gray. (B) A close-up view of the central part of the molecule in panel (A), with side chains of the selected residues shown as sticks.

polyphosphates (Ap_nA, with $n \geq 4$) activate it.[13,14] In accordance with the opposite effects of AMP and Ap_4A on CBS-PPase activity, their complexes with the regulatory insert show significant differences in the 3D structure.[12] The pathways through which these structural changes propagate from the regulatory domains to the catalytic site in CBS-PPase still remain to be determined.

CBS-PPase regulation additionally involves a communication between the catalytic sites and the regulatory sites, as indicated by positive cooperativity of substrate hydrolysis (kinetic cooperativity) and monoadenosine-phosphate binding.[15] Accordingly, two different Michaelis and nucleotide-binding constants are required to describe the hydrolysis kinetics and its modulation by monoadenosine phosphates, respectively. Ap_4A is unique as a regulator of CBS-PPase because it bridges two Bateman modules in the enzyme dimer[12] and, hence, binds noncooperatively. A less predictable effect of Ap_4A is that it abolishes kinetic cooperativity,[14] which can be explained in two principally different ways: the dinucleotide either blocks communication between the catalytic sites and allows them to function independently or "silences" one active site (ultimate kinetic cooperativity). Interestingly, CBS-PPase is the only known CBS-protein regulated by diadenosine polyphosphates, acting as cellular alarmones.[16]

Recent studies have identified two residues (Asn312 and Arg276) that are located in the DHH and CBS domains, respectively, and have a prominent role in CBS-PPase regulation and catalysis.[17,18] Asparagine substitution by a serine residue dramatically affects regulation by abolishing kinetic cooperativity in the absence of adenine nucleotides but restoring it in the presence of Ap_4A.[17] The arginine located in the CBS2 domain has been found to control kinetic cooperativity, nucleotide-binding affinity, and the size of the regulatory signal exerted by both mono- and dinucleotides.[18] However, transmission of the regulatory signal from the CBS domains to a distantly located catalytic site and between subunits in CBS-PPase should involve an extended residue network that links all catalytic and regulatory sites in CBS-PPase. To identify other members of the network, we performed an extensive mutagenesis study of the subunit interface-forming CBS and DHH domains. The results reported below confirmed the proposed role of Asn312 and identified two arginine residues, Arg295 and Arg334, with a prominent role in activity regulation.

RESULTS

Selection of Residues for Substitution. Polar residues potentially important for signal transduction between the regulatory and active sites in *dh*PPase were selected based on two criteria: location in the contact regions of secondary structure elements and a high degree of conservation in CBS-PPases. The tertiary structures of the catalytic and regulatory parts of *dh*PPase were obtained by homology modeling using canonical *Bacillus subtilis* PPase[10] in the "open" conformation and the regulatory part of *cp*PPase[12] with bound AMP as the templates, respectively. The two parts were thereafter combined into a full-size structure (Figure 1), as described previously for *cp*PPase.[12] Regulatory ligand-binding residues in CBS domains generally belong to β-strands, whereas α-helices transmit the ligand-induced conformational change to catalytic domains.[1,2] The structural analysis suggested that helix α1 (residues 266−275) is the best candidate for signal transmission to the catalytic DHH domain. This helix interacts with the loops formed by residues 310−323 and 334−341; the former loop contains Asn312, earlier shown to be important for catalysis and kinetic cooperativity.[17] Next to the other side of helix α1 is Arg276, also important for allosteric regulation.[18]

Sequence comparison of 188 CBS-PPase sequences retrieved by a BLAST search of the NCBI Protein and KEGG GENES databases indicated high conservation in the regions suggested by the 3D model to be important for signal transduction between the CBS2 and DHH domains (Figure S1). Of note, the overall degree of conservation was smaller for the regulatory domain in comparison with the catalytic one (27 vs 49%[8]). Based on the two criteria, six residues were selected for mutagenesis: CBS2 domain Ser266, Glu267, Lys269, and Arg295 and DHH domain Asn312 and Arg334 (Figure 1B). Residues 266, 267, and 269 belong to helix α1, and residue 295 belongs to helix α2 of the CBS2 domain. Asn312 of the DHH

DOI: 10.1021/acsomega.9b01879
ACS Omega XXXX, XXX, XXX−XXX

Table 1. Effects of Adenine Nucleotides on the Activities of *dh*PPase Variants Measured at 50 μM $MgPP_i$ and 5 mM Free Mg^{2+}[a]

		v_N/v				
enzyme	$v/[E]_0$ (s^{-1})	AMP	ADP	ATP	Ap_4A	Ap_5A
wild type[b]	110 ± 4	0.037 ± 0.001	0.09 ± 0.01	2.5 ± 0.2	3.8 ± 0.1	3.32 ± 0.06
S266A	85 ± 2	0.07 ± 0.02	0.23 ± 0.03	1.5 ± 0.1	1.5 ± 0.1	3.7 ± 0.1
S266D	76 ± 2	0.03 ± 0.01	0.03 ± 0.01	2.5 ± 0.2	2.6 ± 0.1	3.6 ± 0.2
E267A	68 ± 1	0.17 ± 0.03	0.05 ± 0.01	2.5 ± 0.2	2.7 ± 0.1	3.6 ± 0.1
K269A	15 ± 0.2	0.15 ± 0.05	0.40 ± 0.07	2.8 ± 0.2	3.5 ± 0.1	3.6 ± 0.2
K269R	38 ± 1	0.03 ± 0.01	0.18 ± 0.02	2.3 ± 0.3	3.0 ± 0.1	4.9 ± 0.5
K269E	21 ± 1	0.016 ± 0.012	0.03 ± 0.01	2.5 ± 0.2	2.46 ± 0.07	4.9 ± 0.4
R295A	0.43 ± 0.01	0.53 ± 0.02	0.47 ± 0.02	**0.63 ± 0.02**	**240 ± 20**	**0.58 ± 0.02**
R295L	3.5 ± 0.1	0.36 ± 0.01	0.38 ± 0.01	**0.42 ± 0.01**	12 ± 1	**0.71 ± 0.03**
R295E	3.2 ± 0.1	0.46 ± 0.01	0.23 ± 0.01	3.9 ± 0.2	**90 ± 10**	**52 ± 1**
N312A	0.68 ± 0.02	0.20 ± 0.04	0.41 ± 0.05	**0.25 ± 0.05**	14 ± 2	9.7 ± 0.4
R334A	5.8 ± 0.2	0.03 ± 0.01	0.38 ± 0.4	4.7 ± 0.2	11 ± 1	7.5 ± 1.0
R334K	27 ± 1	0.009 ± 0.007	0.045 ± 0.007	2.5 ± 0.1	3.5 ± 0.1	4.7 ± 0.2
R334E	<0.2					

[a]Monoadenosine and diadenosine phosphates were used at 200 and 10 μM, respectively. v_N and v are hydrolysis rates measured in the presence and absence of the nucleotide, respectively. Large effects are indicated by boldface. [b]From ref 15.

domain was earlier found to be involved in kinetic cooperativity (active site interaction),[17] and Arg334 immediately follows the invariant DHH motif (which gave name to the domain), containing two His residues directly involved in catalysis.[19] In some CBS-PPases, Arg334 is conservatively replaced by lysine. None of the selected residues forms contacts with the bound nucleotide in the regulatory site and substrate or metal ions in the active site.

All selected residues were replaced by alanine, and four residues were additionally subjected to more drastic (Ser/Asp, Lys/Glu, Arg/Glu) or less drastic (Lys/Arg, Arg/Lys) substitutions (Table 1). Arg295 was additionally replaced by Leu, frequently found in this position in naturally occurring CBS-PPases.

Production and Structural Characterization of *dh*PPase Variants. Wild-type *dh*PPase and its variants were produced in *Escherichia coli* BL21(DE3) cells using the pET expression system. The recombinant proteins gave separate intense bands on SDS-PAGE analysis of cell extracts, indicating successful expression. The variant *dh*PPases were isolated from the extracts by metal affinity chromatography followed by gel filtration. As in previous isolations, the elution profile at the final purification step demonstrated two major peaks, both containing the target variant, which was in an aggregated form in the first peak. Accordingly, only the second peak was collected and used in the studies described below. Typical protein yields were approximately 10 mg/1 L cell culture, and the proteins were >95% pure.

To estimate the effects of the substitutions on the overall structure of *dh*PPase, thermal stability of all alanine variants was measured using the SYPRO Orange dye as a probe for protein unfolding.[20] Five of the six variants exhibited the values of the "melting" temperature, which were derived from the fluorescence versus temperature curves (Figure S2A), similar to or greater than that for the wild-type enzyme (57 ± 1 °C) (Table S1). One variant (K269A) demonstrated a slightly lower melting temperature (54 ± 1 °C).

Sedimentation velocity measurements of the six alanine variants indicated no significant changes in the $s_{20,w}$ value (Table S2) and, hence, the oligomeric structure. The fraction of the aggregated forms with masses exceeding that for the dimer was the highest in the E267A variant (19%) and did not exceed 10% in other cases.

General Characterization of Adenine Nucleotide Effects on *dh*PPase Variants. AMP and ADP inhibit, whereas ATP and diadenosine polyphosphates activate wild-type *dh*PPase.[14,15] For the initial characterization of the variant *dh*PPases, the effects of these modulators on activity were screened at fixed concentrations that were saturating for the wild-type enzyme and a fixed concentration of the substrate (50 μM). All *dh*PPase variants retained the ability to be inhibited by AMP and ADP, although the degree of inhibition was smaller in many cases (Table 1). Most variants similarly retained their ability to be activated by ATP and diadenosine polyphosphates, with few notable exceptions. Most surprisingly, two Arg295 substitutions converted both ATP and Ap_5A from activators into inhibitors, and the Asn312 substitution converted ATP into an inhibitor. Not less surprisingly, the degree of activation by Ap_4A increased by two orders of magnitude upon the R295A and R295E substitutions. Activation by Ap_5A was similarly enhanced by the R295E but not by the R295A substitution. A more detailed analysis of the effects of three nucleotides (AMP, Ap_4A, and ATP) measured at varied nucleotide and substrate concentrations is described below. The activity of the R334E variant was quite low, and it was not characterized further.

Detailed Analysis of AMP, Ap_4A, and ATP Effects at a Fixed Substrate Concentration. In this section, we measured the effects of the three nucleotides in wide ranges of their concentrations and analyzed the results in terms of Scheme 1 and eq 1 with unequal K_N values for two binding sites in the enzyme dimer. We also characterized the degree of binding cooperativity with the Hill coefficient, h, of the empirical eq 3. The values of the ratio K_{N1}/K_{N2} and h exceed unity for positive cooperativity and are less than unity for negative cooperativity; the expected maximal value of h for dimeric CBS-PPase is two, whereas the K_{N1}/K_{N2} ratio may adopt any value. The advantage of the microscopic binding constants over the Hill coefficient is that they allow for a more quantitative description of the cooperativity phenomenon.[21] The corresponding dose dependencies for the alanine variants are presented in Figure 2, and the parameter values derived

DOI: 10.1021/acsomega.9b01879
ACS Omega XXXX, XXX, XXX−XXX

Scheme 1. Kinetic Scheme Describing Adenine Nucleotide Effects on a Dimeric Enzyme E_2 with Two Regulatory Sites at a Constant Substrate Concentration[a]

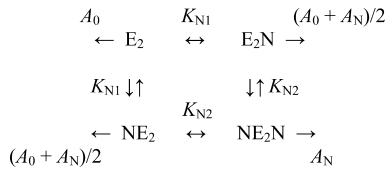

[a]N is the nucleotide, K_{N1} and K_{N2} are the microscopic nucleotide-binding constants, and A_0 and A_N are the activities ($v/[E]_0$) of the nucleotide-free and nucleotide-bound subunits, respectively. E_2 represents the sum of substrate-free and substrate-bound enzyme forms.

therefrom with eq 1 are summarized in Figure 3 (see also Tables S3–S5 for numerical data), along with analogous data for other variants.

All variants were inhibited by AMP (Figures 2A and 3A; see also Table S3), but the inhibition index (A_N/A_0) was markedly elevated in some of them compared to the wild-type enzyme, consistent with the data in Table 1 measured at a nearly saturating concentration of AMP. Most variants retained the positive AMP binding cooperativity (K_{N1}/K_{N2} and $h > 1$) observed in the wild-type *dh*PPase.[15] In two Arg295 replacements, cooperativity was abolished (R295A) or nearly so (R295E). Several variants (S266D, K269E, and N312A) demonstrated enhanced cooperativity, as indicated by the Hill coefficient approaching its upper limit for a homodimeric enzyme. The midpoint AMP concentration on the binding curve ($\sqrt{K_{N1}K_{N2}}$) was greatly reduced in the R295A and R295L variants but elevated in the R295E variant.

The effects of Ap_4A on activity were characterized in a similar way. The limiting values of the activation index (A_N/A_0), obtained by extrapolating activity measured at 50 μM substrate to an infinite Ap_4A concentration (Figure 3A; see also Table S4), did not differ significantly from the v_N/v values found in Table 1, indicating that the 10 μM Ap_4A concentration used in the latter case was saturating or nearly so. Indeed, the K_N values for all *dh*PPase forms lie in the submicromolar range. Ap_4A activated all variant *dh*PPases ($A_N/A_0 > 1$), but five variants (R295L, N312A, R334A, R295A, and R295E in particular) were activated to a much greater extent in comparison to the wild-type enzyme. In all cases, Ap_4A binding appeared to be noncooperative; small apparent deviations in K_{m1}/K_{m2} and h from unity may be associated with the tightness of binding, which required the use of very low Ap_4A concentrations, making the activity assay less accurate.

ATP effects were analyzed for only three variants that demonstrated a reversal of the modulation from activation to inhibition in Table 1. The corresponding dose dependences of the inhibition are shown in Figure 2C, and the results of their analysis are summarized in Figure 3 (see also Table S5). Both Arg295 replacements reversed the ATP-binding cooperativity from positive to negative and slightly tightened ATP binding in terms of $\sqrt{K_{N1}K_{N2}}$. The N312A variant, whose activity was most sensitive to ATP (Figure 3), retained the positive binding cooperativity of the wild-type enzyme.

Effects of the Substitutions on Kinetic Cooperativity in the Absence and Presence of AMP, Ap_4A, and ATP. Rate dependences on substrate concentration for wild-type *dh*PPases and the majority of its variants demonstrated deviations from the Michaelis–Menten equation, that is, "kinetic cooperativity", which could be adequately described in terms of Scheme 2 and eq 2 with unequal K_m values for two active sites in the enzyme dimer (Figure 4). The degree of the kinetic cooperativity was similarly characterized by the ratio K_{m1}/K_{m2} and the Hill coefficient, h (values of the latter parameter are found in Table S6).

Based on these criteria, wild-type *dh*PPase exhibits appreciable positive kinetic cooperativity ($K_{m1}/K_{m2} = 10$, $h = 1.29$).[15] The replacements of Ser266, Glu267, Lys269, and Arg295 had only small effects on the cooperativity, whereas the replacements of Asn312 and Arg334 abolished or markedly decreased it (Figure 5A; see also Table S6). There was no obvious correlation between the effects on cooperativity and individual K_m values; however, K_{m2} was more frequently affected. The largest effect on the mean K_m value ($\sqrt{K_{m1}K_{m2}}$) was observed with the R295A and R295E variants. According to the effects on k_{cat}, the variants can be divided into two groups, that is, those with large effects (boldfaced in Table S6) and those with small or moderate effects. For two residues (Arg295 and Arg334), the effect on k_{cat} strongly depended on the replacing residue.

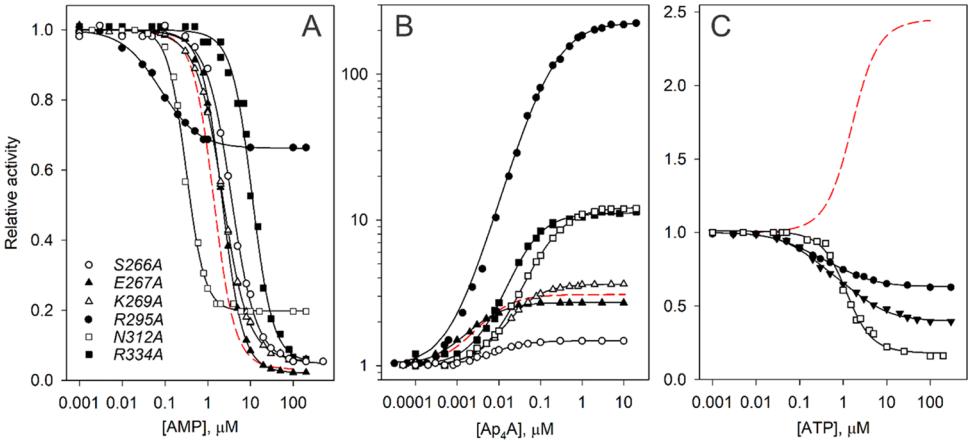

Figure 2. Dependences of the activities of *dh*PPase variants on (A) AMP, (B) Ap_4A, and (C) ATP measured at 50 μM $MgPP_i$ and 5 mM free Mg^{2+}. Activity measured in the absence of any nucleotide was taken as unity in each curve. The lines show the best fits of eq 1. Symbols for all panels are defined in panel (A). The red dashed curves refer to wild-type *dh*PPase and are taken from ref 15 (panels (A) and (C)) or 14 (panel (B)).

DOI: 10.1021/acsomega.9b01879
ACS Omega XXXX, XXX, XXX–XXX

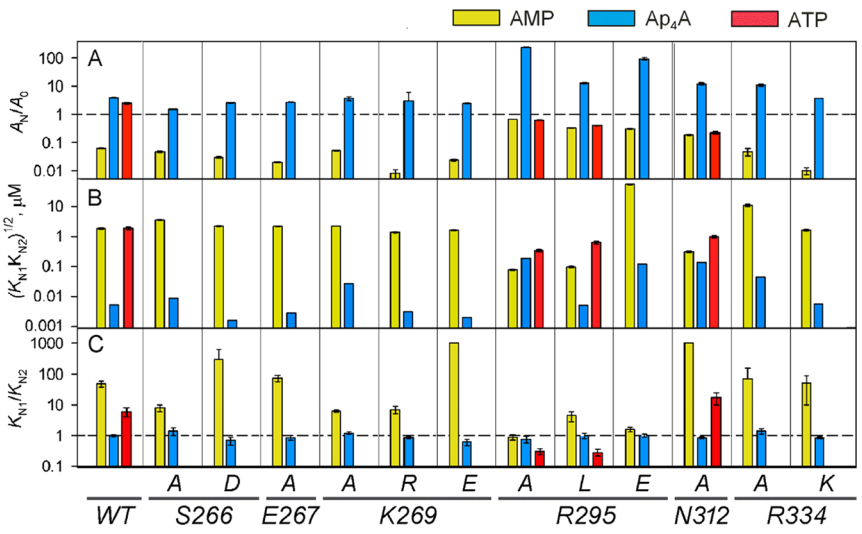

Figure 3. Summary of the effects of residue substitutions on various parameters referring to *dh*PPase regulation by adenine nucleotides: (A) A_N/A_0, (B) $(K_{N1}K_{N2})^{1/2}$, and (C) K_{N1}/K_{N2}. The substituted and replacing residues are indicated in a one-letter notation at the bottom of the figure. The vertical axes are scaled logarithmically. Values measured in the presence of various nucleotides are indicated by different colors detailed at the top of the figure. Dashed horizontal lines mark the parameter level corresponding to the lack of effect (in panel (*A*)) or noncooperative binding (in panel (C)).

Scheme 2. Kinetic Scheme for the Reaction Catalyzed by a Homodimeric Enzyme E_2 with Two Active Sites at a Zero or Fixed Nucleotide Concentration[a]

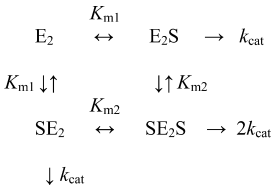

[a]S is the substrate, K_{m1} and K_{m2} are the Michaelis constants, and k_{cat} is the catalytic constant for each active site.

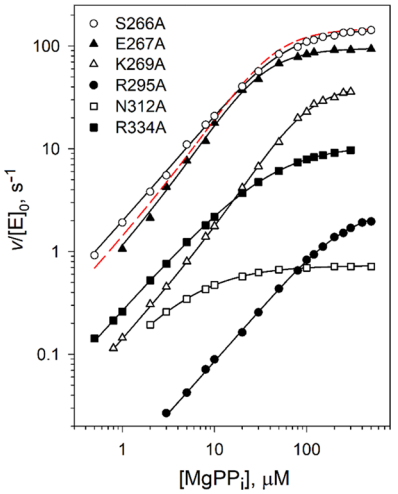

Figure 4. Dependences of the activities of *dh*PPase variants on substrate concentration measured at 5 mM free Mg^{2+}. The lines show the best fits of eq 2. The red dashed curve refers to wild-type *dh*PPase and is taken from ref 15.

In the second set of experiments, we evaluated the effect of fixed concentrations of AMP, Ap_4A, and ATP on the dependences of activity on substrate concentration (Figure S3). This type of experiment with AMP could be performed only with the variants showing reasonably high AMP-binding affinity and a high A_N/A_0 ratio (Figure 3; see also Table S3) because otherwise the nucleotide-free enzyme, present at equilibrium with the nucleotide-bound enzyme, would contribute significantly to the measured activity. ATP effects were again analyzed for the three variants that demonstrated a reversal of the modulation effect in Table 1.

The results of this analysis indicate that AMP decreased the k_{cat} value for all variants (Figure 5A; see also Table S7), that is, it acted as an inhibitor. The effects of AMP on the midpoint substrate concentration on activity versus the $[MgPP_i]$ profile ($\sqrt{K_{m1}K_{m2}}$) were not uniform (Figure 5B; see also Table S7): in most variants, AMP increased $\sqrt{K_{m1}K_{m2}}$, that is, it also acted as an inhibitor, but in the R295A, R295E, and N312A variants, AMP decreased $\sqrt{K_{m1}K_{m2}}$ several fold, that is, it acted as an activator. It should be noted, however, that the activating effect of AMP on the three latter variants only partially compensated for the much larger effects on k_{cat}, which made AMP an inhibitor at any substrate concentration. Interestingly, AMP abolished positive kinetic cooperativity in one variant (R295E) and changed it to slightly or moderately negative in four variants (E267A, R295A, N312A, and R334A) (Table S7).

The effects of Ap_4A on the substrate concentration dependences of activity indicated that Ap_4A increased the k_{cat} value of all variants, except for S266A, by a factor varying from 1.3 to 45 (Figure 5A and Table S8). The effects of Ap_4A on the $\sqrt{K_{m1}K_{m2}}$ values were also favorable for activity, except for the R295A, R295L, and N312A variants, and varied from 7- to 36-fold, that is, it also markedly exceeded the effect on the wild-type enzyme (a 2.4-fold decrease in $\sqrt{K_{m1}K_{m2}}$). As a combined result of the effects of Ap_4A on k_{cat} and $\sqrt{K_{m1}K_{m2}}$, the activities of the R295A and wild-type enzymes measured with 50 μM substrate in the presence of Ap_4A were similar, although their activities measured in the absence of Ap_4A differed by a factor of 250 (Table 1).

A remarkable effect of Ap_4A on the wild-type *dh*PPase was the abolishment of kinetic cooperativity.[14] This property was retained in a half of the variants, whereas the other half

DOI: 10.1021/acsomega.9b01879
ACS Omega XXXX, XXX, XXX−XXX

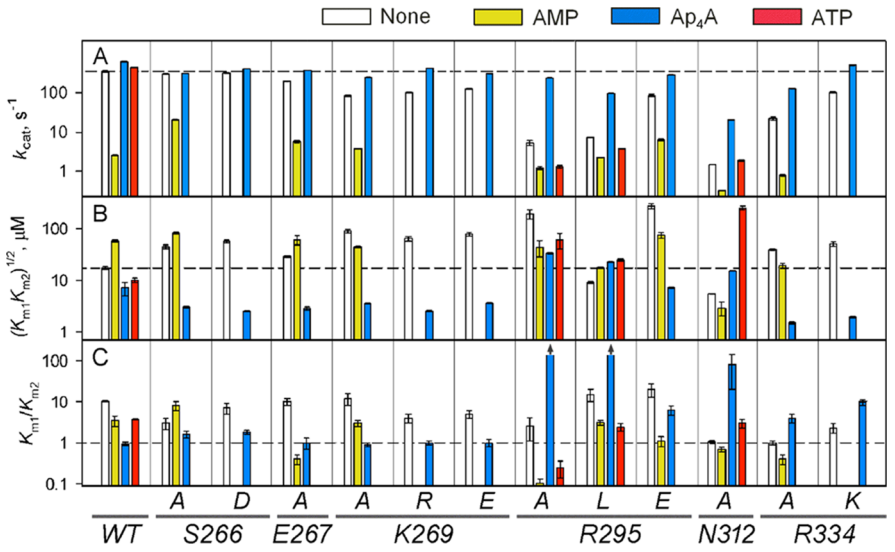

Figure 5. Summary of the effects of residue substitutions on various parameters describing $MgPP_i$ hydrolysis by *dh*PPase in the absence and presence of adenine nucleotides: (A) k_{cat}, (B) $(K_{m1}K_{m2})^{1/2}$, and (C) K_{m1}/K_{m2}. The substituted and replacing residues are indicated in a one-letter notation at the bottom of the figure. The vertical axes are scaled logarithmically. Bars showing the values that exceeded the ordinate range in panel (C) end with arrows. Values measured in the presence of various nucleotides are indicated by different colors detailed at the top of the figure. Dashed horizontal lines mark the parameter level for nucleotide-free wild-type *dh*PPase (panels (A) and (B)) or for noncooperative kinetics (panel (C)).

demonstrated positive kinetic cooperativity (Figure 5C), the degree of which generally exceeded that demonstrated by the wild-type enzyme in the absence of any nucleotide. For two Arg295 replacements, the Hill coefficient even reached its limiting value for a dimeric enzyme (Table S8).

ATP reversed kinetic cooperativity only in the R295A variant, while two other tested variants (R295L and N312A) retained the positive cooperativity of the wild-type enzyme (Figure 5C; see also Table S9). ATP activation of the wild-type enzyme resulted from favorable changes in both k_{cat} (an increase) and $\sqrt{K_{m1}K_{m2}}$ (a decrease). In the R295L variant, the ATP effects on both parameters were unfavorable for activity, whereas in the two other variants, ATP induced an unfavorable change in one parameter and a favorable change in the other. Of note, the R295A variant was inhibited by ATP at any substrate concentration because the unfavorable effect on k_{cat} exceeded that of the favorable effect on $\sqrt{K_{m1}K_{m2}}$, whereas the N312A variant was slightly activated in saturating conditions but inhibited at low substrate concentrations (compare the N312A curves in Figure 4 and Figure S3C).

Modeling and MD Simulations. We have previously modeled a three-dimensional structure of an N77S variant of canonical family II PPase from *B. subtilis*[17] to understand why a corresponding mutation (N312S) abolished active site interaction (kinetic cooperativity) in *dh*PPase. The modeled structure contained a bound substrate analogue, imidodiphosphate, in only one subunit to mimic the state at which substrate binding cooperativity is manifested. Here, we performed the same modeling for the N77A variant of *B. subtilis* PPase. The modeled structure (Figure 6B) indicated an even more drastic change in the H-bonding pattern of the loop formed by residues 96−109 at the subunit interface. The replacement predictably caused loss of all intrasubunit bonds of the residue 77 side chain. As a consequence, only three intersubunit H-bonds were detected with the program Hbonanza[22] using default settings in the N77A variant—between Arg99 and Thr105′ (Nε2···O), between Asn102 and Phe103′ (N···O), and between Thr105 and Ile100′ (Oγ···N) (Figure 6B) compared with eight such H-bonds present in the wild-type enzyme (Figure 6A).

Modeling was also performed for the *B. subtilis* PPase R99A variant, which corresponds to the R334A variant of *dh*PPase used in this study. Unlike Asn77, Arg99 interacts directly with the other subunit. Again, only three intersubunit H-bonds were detected (Figure 6C), but they differed from those in the N77A variant. These H-bonds included those between Ile100 and Thr105′ (N···Oγ and O···N) and between Phe103 and Ile100′ (N···O). Interestingly, Asn77 lost most of its intrasubunit H-bonds as a result of the R99A substitution, resembling the effects of the N77A substitution. Thus, these two mutations similarly destabilized the contact region of the DHH domains in *B. subtilis* PPase.

Both simulated structures slightly differed from the crystal structure of the wild-type enzyme (Figure S4). However, the differences were of the same size as observed previously for wild-type *bs*PPase[17] and seemingly result from structural distortions of the crystalline state.

DISCUSSION

The regulatory and catalytic sites are separated in space in CBS-PPase (Figure 1). Therefore, signal transfer between the sites requires coordinated movements of multiple amino acid residues. In terms of the "induced-fit" concept,[23] the resting regulatory site does not perfectly fit the nucleotide molecule to be bound, so the binding event involves the displacement of protein ligands to establish all interactions with the nucleotide. To generate a regulatory signal, part of these interactions should act like a loaded spring and hence destabilize the complex. As a corollary, replacement of the corresponding amino acid residue with a neutral one, like alanine, should (a) stabilize the complex and (b) suppress or cancel regulation. Furthermore, this "spring" should extend to the active site to transmit the regulatory signal to its destination, and hence, the above predictions are also valid for all spring-forming residues.

DOI: 10.1021/acsomega.9b01879
ACS Omega XXXX, XXX, XXX−XXX

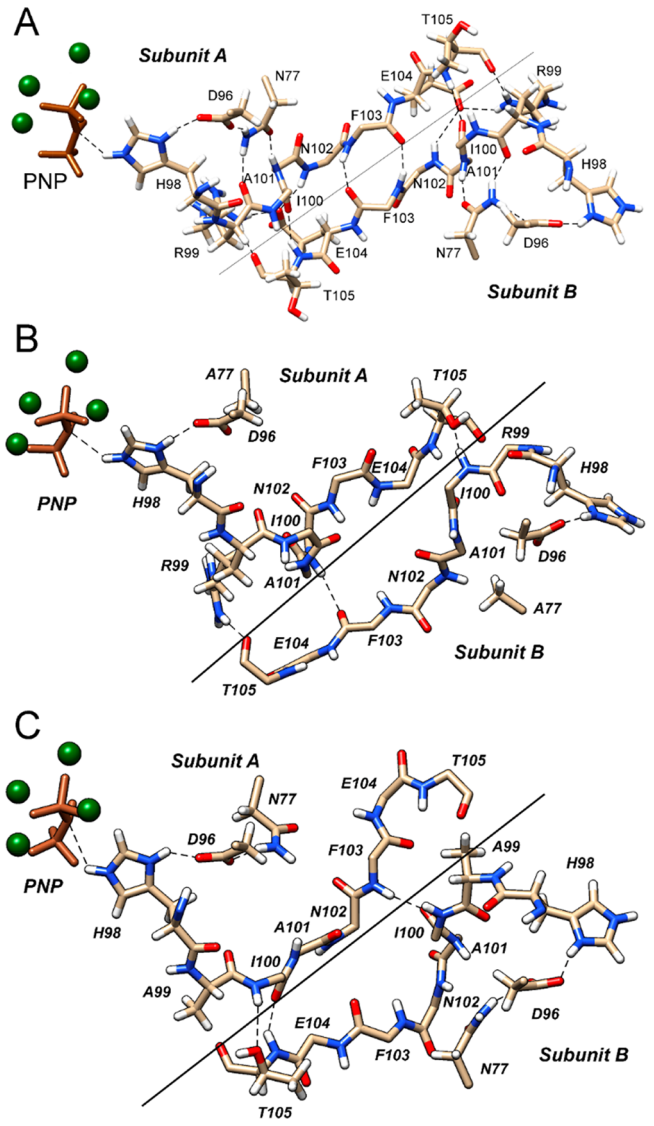

Figure 6. Hydrogen bonding of loop 96−109 and nearby residues at the subunit interface in the simulated structures of (A) the wild-type *B. subtilis* PPase and (B) its N77A and (C) R99A variants, corresponding to *dh*PPase N312A and R334A variants. The H-bonds shown were observed in more than 50% of snapshots saved during the 650−700 ns interval. The solid line separates subunits A and B. The imidodiphosphate (PNP) molecule (orange sticks) and four Mg^{2+} ions (green spheres) are bound in the active site of subunit A; subunit B contains only two Mg^{2+} ions (not shown). The figure in panel (A) was taken with permission from ref 17.

None of the residues substituted in this study is a nucleotide ligand, disallowing direct inferences on where the spring starts. However, the data in Figure 3A,B identify two intermediate residues with the predicted effects of the mutation—Arg295 and Asn312. Indeed, the mutation of Arg295 to Ala or Leu decreased the mean binding constant, $\sqrt{K_{N1}K_{N2}}$, for AMP by approximately 20-fold and increased the residual activity of the AMP complex 5−10-fold. These mutations exerted similar, although smaller effects on the strength of ATP binding, cancelling or even reversing its activating effect (Figure 3A). The Asn312A replacement had similar effects on the binding of AMP and ATP and their modulating effects on activity (Figure 3A,B). The correlation between the effects of the substitutions on the regulation by AMP and ATP suggests that ligand-mediated inhibition and activation are transmitted through the same residues. One can further speculate that the inhibiting nucleotides increase the strain in the spring, whereas the activating nucleotides partially release it.

Our previously published data on the N312S variant of *dh*PPase[17] are fully consistent with these inferences. The substitution decreased $\sqrt{K_{N1}K_{N2}}$ for AMP binding by approximately 4-fold and increased the residual activity of the complex by 10-fold. In contrast, the R276A substitution increased the residual activity of the AMP complex by 13-fold,[18] as expected for a spring-forming residue, but had a different effect on $\sqrt{K_{N1}K_{N2}}$ for AMP (a 12-fold increase). Similar effects on AMP binding and regulation were previously observed upon R168A and R187G substitutions in the DRTGG domain-lacking *Moorella thermoacetica* CBS-PPase,[24] wherein Arg168 and Arg187 correspond to *dh*PPase Arg276 and Arg295, respectively.

Regulation of CBS domain-containing enzymes and transporters by nucleotides is attributed to their modulation of the internal inhibition imposed by the CBS domains on protein function.[25] Several lines of evidence support this concept in the case of CBS-PPase. They include the findings that CBS-PPases exhibit a diminished activity (by one to three orders of magnitude) compared with their close homologues lacking CBS domains[26] and that nucleotides may inhibit (AMP and ADP) or activate (ATP and diadenosine polyphosphates) this enzyme. Furthermore, several mutations in CBS domains activated CBS-PPase of *M. thermoacetica* and some even reversed the effect of nucleotide from inhibition to activation,[24] resembling the effects of mutations in cystathionine β-synthase[27] and AMP-dependent protein kinase.[28,29] Finally, deletion of the regulatory domains in *dh*PPase favorably changed (decreased) its K_m values.[15]

The results of this study support and further extend the concept of internal inhibition induced in CBS-PPase by the regulatory insert. In terms of the mechanical model of CBS-PPase regulation, internal inhibition is caused by a strain at the interface of the regulatory and catalytic domains, which is transmitted to the active site and distorts it. The pathways through which the signals from the regulatory insert itself and bound nucleotides reach the active site seem both involve Arg295 and Asn312 and hence overlap, at least partially. This inference comes from the finding that Arg295 modifications suppressed catalytic activity by two orders of magnitude and simultaneously enhanced its activation by Ap_4A, such that the activity of the Ap_4A-activated R295A and R295E variants was comparable with the activity of the wild-type enzyme. Of note, these findings add to the knowledge that, despite the low activity of the variant enzymes, the substitutions did not disrupt the protein structure. Apparently, the substitutions aggravated the internal inhibition by CBS domains, but this effect was largely reversed by Ap_4A binding. Furthermore, we found that the removal of the charged side chain in Arg295 or the polar side chain in Asn312 converted ATP from an activator to an inhibitor. The Arg295 modification similarly reversed the activating effect of Ap_5A (Table 1).

Cooperativity of monoadenosine phosphate binding suggests that another spring joins the CBS domains of two subunits in dimeric CBS-PPase. DRTGG domains do not appear to be involved in nucleotide-binding cooperativity, as this has also been exhibited by the CBS-PPases, which lack DRTGG domains in their structures.[15] Only Arg295 but not Asn312 or any other replaced residue is involved in this type of

DOI: 10.1021/acsomega.9b01879
ACS Omega XXXX, XXX, XXX−XXX

Table 2. Summary of the Effects of the Residue Substitutions on the Regulatory Properties of *dh*PPase[a]

	kinetic cooperativity			Michaelis constants			nucleotide-binding cooperativity		nucleotide-binding affinity		degree of inhibition/activation	
enzyme variant	N	M	D	N	M	D	M	D	M	D	M	D
S266A	−	−	−	−	−	−	−	−	−	−	−	−
S266D	−	?	−	−	−	−	−	−	−	−	−	−
E267A	−	++	−	−	−	−	−	−	−	−	−	−
K269A	−	−	−	+	−	−	−	−	−	−	−	−
K269R	−	?	−	−	?	−	−	+	−	−	−	−
K269E	−	?	−	−	?	−	+	−	+	−	−	−
R276A[b]	++	++	++	+	++	−	−	?	−	−	+	+
R276K[b]	+	++	++	−	+	−	−	−	−	−	−	−
R276E[b]	−	−	+	+	−	−	+	−	+	−	−	−
R295A	−	++	++	+	−	++	++	−	++	+	++	++
R295L	−	−	++	−	−	++	++	−	+	+	++	−
R295E	−	++	+	+	−	−	+−	−	−	+	+	++
N312A	++	++	++	+	++	+	+	−	+	+	++	−
N312S[c]	++	++	++	+	++	−	+	−	+	++	++	+
R334A	++	++	+	−	−	−	−	−	−	+	−	−
R334K	−	?	++	?	−	−	−	−	−	−	−	−

[a]A minus sign (−) indicates small or no effect, plus sign (+) indicates a large effect, two plus signs (++) indicate a profound effect, and question mark (?) indicates lack of information. Columns marked as N, M, and D refer to the effects measured without any nucleotide, in the presence of the mononucleotides, and in the presence of the dinucleotides, respectively. [b]From ref 18. [c]From ref 17.

cooperativity, as it was appreciably suppressed or, ultimately, reversed only upon the removal of the Arg295 guanidino group (Figure 3C). In contrast, replacements of Asn312 (N312A and N312S) dramatically increased the cooperativity of AMP binding (Table S3 and ref 17), which may mean that Asn312 interactions counteract this type of cooperativity. The effect of the Asn312 substitutions on ATP binding was much smaller, if any (Table S5). Ap_4A bound noncooperatively in wild type and all variant *dh*PPases, consistent with its binding stoichiometry of 1 mole/mole dimer.[12,14]

Yet another spring connects active sites in CBS-PPase, causing positive kinetic cooperativity, as manifested by the decreased Michaelis constant for the second bound substrate molecule. We found earlier that this type of cooperativity was eliminated by the N312S substitution.[17] The importance of Asn312 for kinetic cooperativity is supported by the N312A data (Figure 5C). Consistent with this, the N312A variant exhibited a lower mean Michaelis constant ($\sqrt{K_{m1}K_{m2}}$) in comparison with the wild-type enzyme (Figure 5B). Furthermore, our new data suggest that Arg334 also plays a role in kinetic cooperativity, as R334A substitution also made the hydrolysis kinetics noncooperative (Figure 5C), despite the fact that it did not decrease $\sqrt{K_{m1}K_{m2}}$. One should keep in mind that this parameter is a combination of rate constants, rather than a binding constant, and its increase does not necessarily imply the increased strain on the spring.

A surprising effect of Ap_4A was to eliminate or greatly decrease kinetic cooperativity in different CBS-PPases[14] and the *dh*PPase variants with substituted Ser266, Glu267, and Lys269 residues (Figure 5C). This may mean that the cross-linking Ap_4A molecule fixes the active site-connecting spring in one position or completely relaxes it, for instance, by disrupting the contact between the catalytic DHH domains. In a sharp contrast, Ap_4A induced a very high positive kinetic cooperativity in the variants with substituted Arg295 and Asn312 residues and less so in the Arg334 variants (Figure 5C). A likely corollary is that a cross-linking Ap_4A molecule somehow restores intersubunit contact through DHH domains or replaces it in the variants with substituted Asn312 and Arg334 residues. However, these interpretations may be inappropriate with the Arg295-substituted variants, as they retained kinetic cooperativity in the absence of nucleotides (Figure 5C). Further structural studies are clearly needed to explain the opposite effects of Ap_4A on kinetic cooperativity in different variants.

The following note is appropriate at the point. A classical view of allosteric effects, including binding cooperativity, implies a conformational change induced by ligand binding to a remote site. However, an increasing body of evidence supports a different, entropic concept that relies upon changes in the dynamic fluctuations about the mean conformation with no change in the mean conformation itself.[30,31] A combination of the "conformational" and "entropic" mechanisms is also possible. Our mechanical description of cooperativity is applicable to both mechanisms, depending to what is assumed to load "springs"—static displacements of atoms or changes in their dynamic behavior.

Because the substrate itself binds cooperatively to CBS-PPase in the absence of nucleotides, the apparent nucleotide binding cooperativity, which was also inferred from activity measurements, might be induced by the bound substrate or by nucleotide-mediated modulation of substrate binding. However, lack of correlation between the effects of the mutations on kinetic and nucleotide binding cooperativities (Figures 3C and 5C) apparently refutes such a mechanism. The absence of a causative link between the cooperativities of binding to two types of sites in CBS-PPase is also consistent with the previous finding that the AMP- and ATP-binding cooperativity in *dh*PPase does not depend significantly on substrate concentration.[15]

Table 2 summarizes the functional consequences of all heretofore described substitutions in the CBS and DHH domain residues that were deemed important for the regulation of CBS-PPase. These data identify four residues that are indeed important: arginines 276, 295, and 334 and asparagine 312. Substitutions of two of these residues, Arg295

DOI: 10.1021/acsomega.9b01879
ACS Omega XXXX, XXX, XXX−XXX

and Asn312, affected practically all parameters associated with the three regulatory signal pathways connecting the active sites, the regulatory sites, and the regulatory and active sites. Noteworthy, *Ethanoligenens harbinense* CBS-PPase, which has leucine and serine in the positions corresponding to *dh*PPase Arg295 and Asn312, respectively, is not regulated by adenine nucleotides and exhibits no kinetic cooperativity.[17] Furthermore, these residues appear to be involved in the internal inhibition imposed by the regulatory domains in the absence of nucleotides. Arg334, like the previously explored Arg276,[18] is essential for signal transduction between the catalytic domains of different subunits. However, Arg334 differs from Arg276 in that it is not involved in signal transduction between the regulatory and catalytic domains within one subunit, as Arg334 substitution with alanine did not appreciably change the effects of nucleotides on activity. Noteworthy, positions 295, 312, and 334 are almost invariant or, rarely, conservatively replaced in hundreds of CBS-PPase sequences (Figure S1).

Modeling and MD simulation experiments on *B. subtilis* PPase, which contains only catalytic DHH and DHHA2 domains in its structure, provided a likely structural explanation for the roles of Asn312 and Arg334 in kinetic cooperativity in *dh*PPase. These experiments indicate that replacements with alanine of the corresponding Asn77 and Arg99 residues destabilize subunit contact through the DHH domains (Figure 6), thus hampering signal transfer between active sites. Modeling the behavior of the Arg295-substituted variants could not be performed in the same way because Arg295 belongs to the CBS domain, not found in *B. subtilis* PPase. It is unlikely that the effect of Arg295 substitution is also associated with the modification of DHH−DHH contact because the Arg295-substituted variants exhibited positive kinetic cooperativity in the absence of adenine nucleotides (Figure 5C). In the structure of the regulatory part of *C. perfringens* CBS-PPase, the guanidino group of the corresponding Arg296 residue forms four H-bonds with other residues, and their disruption by R/A or R/L mutation may have an unpredictable effect on the enzyme structure and function.

In conclusion, our data define the roles for two amino acid residues, Arg295 and Arg334, as important in the activity regulation of CBS-PPase and support the previously assigned role of Asn312 in regulation. In more general terms, the results of this study attest to the usefulness of CBS domain-containing pyrophosphatase as a model enzyme to study the general principles of protein regulation via CBS domains, at the same time emphasizing a critical requirement for the structure of a full-size enzyme for further progress.

EXPERIMENTAL SECTION

Materials. Wild-type *dh*PPase (UniProtKB: B8FP42) and its variants containing a His_6 tag at their N-termini were isolated from *E. coli* BL21 cells transformed with the pET-28b vector (Novagen) carrying the corresponding gene, as described previously.[18] Site-directed mutagenesis was performed using overlap extension PCR with Phusion DNA polymerase. The purity of the final products was estimated by SDS-PAGE[32] with Coomassie staining. Protein concentrations were determined spectrophotometrically, using an $A^{0.1\%}_{280}$ value of 0.477, as calculated from the amino acid composition with ProtParam. Molar concentrations were calculated on the basis of a subunit molecular mass of 62.5 kDa for the His_6-tagged protein.

AMP (free acid), ADP (diammonium salt), ATP (disodium salt), Ap_4A (ammonium salt), and Ap_5A (pentasodium salt) were obtained from Sigma-Aldrich. The concentrations of nucleotide stock solutions were estimated by measuring absorbance at 259 nm (ε = 15,900 M^{-1} cm^{-1} for the mononucleotides and 31,800 M^{-1} cm^{-1} for the dinucleotides).

Kinetic Assays. The activity assay medium contained 5 mM free Mg^{2+} ion (added as $MgCl_2$), 50 μM $MgPP_i$ complex (added as tetrasodium PP_i), and 0.1 M Tes-KOH or Mops-KOH buffer, pH 7.2, except where specified otherwise. Reactions were initiated by adding an enzyme, and P_i accumulation due to PP_i hydrolysis was continuously recorded for 2−3 min at 25 °C using an automated P_i analyzer[33] at a sensitivity of 4−20 μM P_i per recorder scale. Initial velocity values were proportional to enzyme concentration and generally agreed within 5−10% in replicate measurements.

Bioinformatics Analysis. CBS-PPase protein sequences were retrieved by BLAST from the NCBI Protein[34] and KEGG GENES[35] databases. Protein sequences were aligned with ClustalX (version 2.1) using default settings. The alignment was manually processed by eliminating incomplete and redundant sequences and sequence regions that included indels and ambiguously aligned residues. Protein structures were visualized and analyzed using UCSF Chimera.[36]

ThermoFluor Measurements.[20] Thermostability measurements were performed using a C1000 thermal cycler with the CFX96 real-time PCR detection system (Bio-Rad). The assay mixtures with a total volume of 50 μL, placed in transparent low-profile 96-well multiplate PCR plates (SSIbio), contained 5−8 μM enzyme, 0.02% SYPRO Orange dye (Invitrogen), 0.1 M Mops-KOH buffer, pH 7.2 (measured at 25 °C), 2 mM $MgCl_2$, 0.1 mM $CoCl_2$, and 150 mM KCl. The plates were closed with an UltraFlux Standard PCR sealing film (SSIbio) and heated from 30 to 100 °C with stepwise increments of 0.5 °C and a 20 s hold step for every point. Fluorescence was monitored at 552 nm (second channel, VIC filter), and melting temperatures, T_m, were determined from the resulting curves with CFX Manager software.

Sedimentation Analysis. Analytical ultracentrifugation was performed at 25 °C in a Spinco E instrument (Beckman Instruments) equipped with a computerized data collection unit, with scanning at 280 nm. Samples contained 10−20 μM CBS-PPase, 0.1 M Mops/KOH buffer, pH 7.2, 2 mM $MgCl_2$, 0.1 mM $CoCl_2$, and 150 mM KCl. Prior to each run, samples were incubated for 6 h at 25 °C. The sedimentation velocity was measured at 60,000 rpm, and sedimentation coefficients ($s_{20,w}$) were calculated with the program SedFit.[37]

Molecular Dynamics (MD). Virtual mutations and molecular dynamics (MD) simulations with dimeric canonical *B. subtilis* PPase, which lacks the regulatory CBS-DRTGG-CBS insert, were carried out essentially as described previously.[17] MD simulations were performed using the PMEMD program (CUDA implementation) of the AMBER 14 software suite with the ff14SB force field (http://ambermd.org/). The 8 Å cutoff production MD simulation was performed for 750 ns for each variant protein, with snapshots saved every 10 ps. Post-processing trajectory analyses were carried out with the program CPPTRAJ of the AMBER 14 pack.

Data Analysis and Calculations. Nucleotides effects on activity at a fixed substrate concentration were analyzed in terms of Scheme 1, written in terms of microscopic binding constants, like in our latest publication.[18] Use of microscopic constants simplified analysis in comparison to the use of

DOI: 10.1021/acsomega.9b01879
ACS Omega XXXX, XXX, XXX−XXX

macroscopic constants in previous analyses[14,15,17] without effect on its results. The microscopic and macroscopic binding (and Michaelis) constants are linked by the following relationships: $K_{N1(micro)} = 2K_{N1(macro)}$, $K_{N2(micro)} = 0.5K_{N2(macro)}$.[38] The dependences of the hydrolysis rate (v_N) on nucleotide concentration ([N]) were fit to eq 1.[18] In the framework of Scheme 1, binding cooperativity can be diagnosed by comparing the K_N constants: $K_{N1} > K_{N2}$ indicates positive cooperativity, $K_{N1} < K_{N2}$ indicates negative cooperativity, and $K_{N1} = K_{N2}$ is indicative of noncooperative behavior. Decreases in the free nucleotide concentration because of binding to the enzyme could be neglected in all cases, except for the pair R295A variant/Ap_4A. In the latter case, eq 1 was fitted to the binding data together with mass balance equations for the enzyme and nucleotide. According to eq 1, the midpoint of the $v/[E]_0$ versus [N] profile is achieved at nucleotide concentration equal to $\sqrt{K_{N1}K_{N2}}$.

$$v_N/[E]_0 = \{A_N + (A_0 + A_N)K_{N2}/[N] + A_0K_{N1}K_{N2}/[N]^2\}/(1 + 2K_{N2}/[N] + K_{N1}K_{N2}/[N]^2) \quad (1)$$

The cooperative kinetics of substrate ($MgPP_i$) hydrolysis is described by Scheme 2, which assumes different microscopic Michaelis constants (K_{m1} and K_{m2}) and equal k_{cat} values for two active sites in the dimer (K-type kinetic cooperativity).[38] The rate equation for Scheme 2 is given by eq 2, where v is the reaction rate, and $[E]_0$ and $[S]$ are the total enzyme and substrate concentrations, respectively.[18] As in the case of nucleotide binding, $K_{m1} > K_{m2}$ implies positive and $K_{m1} < K_{m2}$ implies negative kinetic cooperativity. According to eq 2, half-maximal activity is achieved at a substrate concentration equal to $\sqrt{K_{m1}K_{m2}}$.

$$v/[E]_0 = 2k_{cat}(1 + K_{m2}/[S])/(1 + 2K_{m2}/[S] + K_{m1}K_{m2}/[S]^2) \quad (2)$$

Alternatively, rate dependences on substrate and nucleotide concentrations were fit to eq 3

$$v/[E]_0 = v_0 + (v_L - v_0)/(1 + K_L/[L]^h) \quad (3)$$

where h is the Hill coefficient, L is S or N, and v_L is the rate at infinite [L].

The total concentrations of $MgCl_2$ and PP_i required to maintain desired concentrations of $MgPP_i$ (actual substrate) and 5 mM free Mg^{2+} ion in the activity assay mixture at pH 7.2 were calculated taking into account the following magnesium complexes: $MgPP_i$, Mg_2PP_i, MgAMP, MgADP, and MgATP.[18] Nonlinear least-squares fittings were performed using the program Scientist (Micromath).

■ ASSOCIATED CONTENT

Supporting Information

The Supporting Information is available free of charge on the ACS Publications website at DOI: 10.1021/acsomega.9b01879.

Plots of sequence alignments, ThermoFluor titration data, and substrate concentration dependences of activity and numerical data used to construct bar plots describing effects of the amino acid replacements on catalysis by and regulation of *D. hafniense* pyrophosphatase (PDF)

Accession Codes

Desulfitobacterium hafniense CBS domain-containing pyrophosphatase: UniProtKB B8FP42.

■ AUTHOR INFORMATION

Corresponding Author

*E-mail: baykov@genebee.msu.su.

ORCID

Alexander A. Baykov: 0000-0002-2495-8200

Author Contributions

V.A.A. designed, performed, and analyzed the experiments and contributed to writing the manuscript. A.S. designed and constructed vectors and expressed and purified proteins. E.O. performed experiments. S.A.K. designed and constructed vectors. I.D.D. performed experiments. R.L. supervised the experiments. A.A.B. analyzed experiments and wrote the manuscript. All authors reviewed the results and approved the final version of the manuscript.

Notes

The authors declare no competing financial interest.

■ ACKNOWLEDGMENTS

The authors thank P.V. Kalmykov and N.N. Magretova for help in sedimentation analyses. This work was supported by the Russian Science Foundation (grant no. 17-74-10191) in the part pertaining to quaternary structure and stability measurements.

■ ABBREVIATIONS

Ap_4A, 5′,5-P1,P4-diadenosine tetraphosphate; CBS, cystathionine β-synthase; CBS-PPase, CBS domain-containing pyrophosphatase; *cp*PPase, *Clostridium perfringens* CBS-PPase; *dh*PPase, *Desulfitobacterium hafniense* CBS-PPase; MD, molecular dynamics; PPase, pyrophosphatase

■ REFERENCES

(1) Baykov, A. A.; Tuominen, H. K.; Lahti, R. The CBS domain: a protein module with an emerging prominent role in regulation. *ACS Chem. Biol.* **2011**, *6*, 1156−1163.

(2) Ereño-Orbea, J.; Oyenarte, I.; Martìnez-Cruz, L. A. CBS domains: ligand binding sites and conformational variability. *Arch. Biochem. Biophys.* **2013**, *540*, 70−81.

(3) Ignoul, S.; Eggermont, J. CBS domains: structure, function, and pathology in human proteins. *Am. J. Physiol. Cell Physiol.* **2005**, *289*, C1369−1378.

(4) Scott, J. W.; Hawley, S. A.; Green, K. A.; Anis, M.; Stewart, G.; Scullion, G. A.; Norman, D. G.; Hardie, D. G. CBS domains form energy-sensing modules whose binding of adenosine ligands is disrupted by disease mutations. *J. Clin. Invest.* **2004**, *113*, 274−284.

(5) Li, J.; Li, S.; Wang, F.; Xin, F. Structural and biochemical insights into the allosteric activation mechanism of AMP-activated protein kinase. *Chem. Biol. Drug Des.* **2017**, *89*, 663−669.

(6) Niu, W.; Wang, J.; Qian, J.; Wang, M.; Wu, P.; Chen, F.; Yan, S. Allosteric control of human cystathionine β-synthase activity by a redox active disulfide bond. *J. Biol. Chem.* **2018**, *293*, 2523−2533.

(7) Young, T. W.; Kuhn, N. J.; Wadeson, A.; Ward, S.; Burges, D.; Cooke, G. D. *Bacillus subtilis* ORF yybQ encodes a manganese-dependent inorganic pyrophosphatase with distinctive properties: the first of a new class of soluble pyrophosphatase? *Microbiology* **1998**, *144*, 2563−2571.

(8) Baykov, A. A.; Anashkin, V. A.; Salminen, A.; Lahti, R. Inorganic pyrophosphatases of Family II—two decades after their discovery. *FEBS Lett.* **2017**, *591*, 3225−3234.

DOI: 10.1021/acsomega.9b01879
ACS Omega XXXX, XXX, XXX−XXX

(9) Merckel, M. C.; Fabrichniy, I. P.; Salminen, A.; Kalkkinen, N.; Baykov, A. A.; Lahti, R.; Goldman, A. Crystal structure of *Streptococcus mutans* pyrophosphatase: a new fold for an old mechanism. *Structure* **2001**, *9*, 289−297.
(10) Ahn, S.; Milner, A. J.; Fütterer, K.; Konopka, M.; Ilias, M.; Young, T. W.; White, S. A. The "open" and "closed" structures of the type-C inorganic pyrophosphatases from *Bacillus subtilis* and *Streptococcus gordonii*. *J. Mol. Biol.* **2001**, *313*, 797−811.
(11) Bateman, A. The structure of a domain common to Archaebacteria and the homocystinuria disease protein. *Trends Biochem. Sci.* **1997**, *22*, 12−13.
(12) Tuominen, H.; Salminen, A.; Oksanen, E.; Jämsen, J.; Heikkilä, O.; Lehtiö, L.; Magretova, N. N.; Goldman, A.; Baykov, A. A.; Lahti, R. Crystal structures of the CBS and DRTGG domains of the regulatory region of *Clostridium perfringens* pyrophosphatase complexed with the inhibitor, AMP, and activator, diadenosine tetraphosphate. *J. Mol. Biol.* **2010**, *398*, 400−413.
(13) Jämsen, J.; Tuominen, H.; Salminen, A.; Belogurov, G. A.; Magretova, N. N.; Baykov, A. A.; Lahti, R. A CBS domain-containing pyrophosphatase of *Moorella thermoacetica* is regulated by adenine nucleotides. *Biochem. J.* **2007**, *408*, 327−333.
(14) Anashkin, V. A.; Salminen, A.; Tuominen, H. K.; Orlov, V. N.; Lahti, R.; Baykov, A. A. Cystathionine β-synthase (CBS) domain-containing pyrophosphatase as a target for diadenosine polyphosphates in bacteria. *J. Biol. Chem.* **2015**, *290*, 27594−27603.
(15) Salminen, A.; Anashkin, V. A.; Lahti, M.; Tuominen, H. K.; Lahti, R.; Baykov, A. A. Cystathionine β-Synthase (CBS) domains confer multiple forms of Mg^{2+}-dependent Cooperativity to Family II pyrophosphatases. *J. Biol. Chem.* **2014**, *289*, 22865−22876.
(16) Varshavsky, A. Diadenosine 5′,5‴-P^1,P^4-tetraphosphate: a pleiotypically acting alarmone. *Cell* **1983**, *34*, 711−712.
(17) Anashkin, V. A.; Salminen, A.; Vorobjeva, N. N.; Lahti, R.; Baykov, A. A. An Asparagine residue mediates intramolecular communication in nucleotide-regulated pyrophosphatase. *Biochem. J.* **2016**, *473*, 2097−2107.
(18) Anashkin, V. A.; Orlov, V. N.; Lahti, R.; Baykov, A. A. An arginine residue involved in allosteric regulation of cystathionine β-synthase (CBS) domain-containing pyrophosphatase. *Arch. Biochem. Biophys.* **2019**, *662*, 40−48.
(19) Fabrichniy, I. P.; Lehtiö, L.; Tammenkoski, M.; Zyryanov, A. B.; Oksanen, E.; Baykov, A. A.; Lahti, R.; Goldman, A. A trimetal site and substrate distortion in a Family II inorganic pyrophosphatase. *J. Biol. Chem.* **2007**, *282*, 1422−1431.
(20) Ericsson, U. B.; Hallberg, B. M.; DeTitta, G. T.; Dekker, N.; Nordlund, P. Thermofluor-based high-throughput stability optimization of proteins for structural studies. *Anal. Biochem.* **2006**, *357*, 289−298.
(21) Forsén, S.; Linse, S. Cooperativity: over the Hill. *Trends Biochem. Sci.* **1995**, *20*, 495−497.
(22) Durrant, J. D.; McCammon, J. A. HBonanza: a computer algorithm for molecular-dynamics-trajectory hydrogen-bond analysis. *J. Mol. Graphics Modell.* **2011**, *31*, 5−9.
(23) Koshland, D. E., Jr. Application of a theory of enzyme specificity to protein synthesis. *Proc. Natl. Acad. Sci. U. S. A.* **1958**, *44*, 98−104.
(24) Jämsen, J.; Tuominen, H.; Baykov, A. A.; Lahti, R. Mutational analysis of residues in the regulatory CBS domains of *Moorella thermoacetica* pyrophosphatase corresponding to disease-related residues of human proteins. *Biochem. J.* **2011**, *433*, 497−504.
(25) Janošík, M.; Kery, V.; Gaustadnes, M.; Maclean, K. N.; Kraus, J. P. Regulation of human cystathionine β-synthase by *S*-adenosyl-L-methionine: evidence for two catalytically active conformations involving an autoinhibitory domain in the C-terminal region. *Biochemistry* **2001**, *40*, 10625−10633.
(26) Parfenyev, A. N.; Salminen, A.; Halonen, P.; Hachimori, A.; Baykov, A. A.; Lahti, R. Quaternary structure and Metal Ion requirement of Family II pyrophosphatases from *Bacillus, subtilis, Streptococcus gordonii* and *Streptococcus mutans*. *J. Biol. Chem.* **2001**, *276*, 24511−24518.
(27) Kery, V.; Poneleit, L.; Kraus, J. P. Trypsin cleavage of human cystathionine β-synthase into an evolutionarily conserved active core: structural and functional consequences. *Arch. Biochem. Biophys.* **1998**, *355*, 222−232.
(28) Adams, J.; Chen, Z.-P.; Van Denderen, B. J. W.; Morton, C. J.; Parker, M. W.; Witters, L. A.; Stapleton, D.; Kemp, B. E. Intrasteric control of AMPK via the γ1 subunit AMP allosteric regulatory site. *Protein Sci.* **2004**, *13*, 155−165.
(29) Barnes, B. R.; Marklund, S.; Steiler, T. L.; Walter, M.; Hjälm, G.; Amarger, V.; Mahlapuu, M.; Leng, Y.; Johansson, C.; Galuska, D.; Lindgren, K.; Åbrink, M.; Stapleton, D.; Zierath, J. R.; Andersson, L. The 5′-AMP-activated protein kinase γ3 isoform has a key role in carbohydrate and lipid metabolism in glycolytic skeletal muscle. *J. Biol. Chem.* **2004**, *279*, 38441−38447.
(30) Cooper, A.; Dryden, D. T. Allostery without conformational change. A plausible model. *Eur. Biophys. J.* **1984**, *11*, 103−109.
(31) Tzeng, S.-R.; Kalodimos, C. G. Protein dynamics and allostery: an NMR view. *Curr. Opin. Struct. Biol.* **2011**, *21*, 62−67.
(32) Laemmli, U. K. Cleavage of structural proteins during the assembly of the head of bacteriophage T4. *Nature* **1970**, *227*, 680−685.
(33) Baykov, A. A.; Avaeva, S. M. A simple and sensitive apparatus for continuous monitoring of orthophosphate in the presence of acid-labile compounds. *Anal. Biochem.* **1981**, *116*, 1−4.
(34) Altschul, S.F.; Gish, W.; Miller, W.; Myers, E. W.; Lipman, D. J. Basic local alignment search tool. *J. Mol. Biol.* **1990**, *215*, 403−410.
(35) Kanehisa, M.; Sato, Y.; Kawashima, M.; Furumichi, M.; Tanabe, M. KEGG as a reference resource for gene and protein annotation. *Nucl. Acids Res.* **2016**, *44*, D457−D462.
(36) Pettersen, E. F.; Goddard, T. D.; Huang, C. C.; Couch, G. S.; Greenblatt, D. M.; Meng, E. C.; Ferrin, T. E. UCSF Chimera - a visualization system for exploratory research and analysis. *J. Comput. Chem.* **2004**, *25*, 1605−1612.
(37) Schuck, P. Size-distribution analysis of macromolecules by sedimentation velocity ultracentrifugation and Lamm equation modeling. *Biophys. J.* **2000**, *78*, 1606−1619.
(38) Bisswanger, H. *Enzyme Kinetics. Principles and Methods*, 2nd ed.; Wiley-VCH Verlag: Weinheim, Germany, 2008.

DOI: 10.1021/acsomega.9b01879
ACS Omega XXXX, XXX, XXX−XXX